Biochemical Pharmacology 83 (2012) 1269–1277

Contents lists available at SciVerse ScienceDirect

Biochemical Pharmacology

journal homepage: www.elsevier.com/locate/biochempharm

Chronic hydrogen-rich saline treatment attenuates vascular dysfunction in spontaneous hypertensive rats

Hao Zheng [a,1], Yong-Sheng Yu [b,1,*]

[a] Department of Pharmaceutical Science and Technology, College of Chemistry and Biology, Donghua University, Shanghai, China
[b] Department of Pharmacology, Second Military Medical University, Shanghai, China

ARTICLE INFO

Article history:
Received 13 November 2011
Accepted 27 January 2012
Available online 9 February 2012

Keywords:
Hydrogen-rich saline
Spontaneously hypertensive rat
Oxidative stress
Vascular dysfunction
Hypertension

ABSTRACT

In hypertensive patients, increased oxidative stress is thought to be one important cause of vascular dysfunction. Recently, it has been suggested that hydrogen exerts a therapeutic antioxidant activity by selectively reducing hydroxyl radical and peroxynitrite, the most cytotoxic chemicals of reactive oxygen species (ROS). Herein, we investigated the protective effect of chronic treatment with hydrogen-rich saline (HRS) against vascular dysfunction in SHR and the underlying mechanism. The 8-week-old spontaneously hypertensive rats (SHR) and age-matched Wistar-Kyoto rats (WKY) were randomized into HRS-treated (6 ml/kg/day for 3 months, i.p.) and vehicle treated group. Treatment with HRS ameliorated vascular dysfunction including aortic hypertrophy and endothelial function in SHR. Treatment with HRS had no significant effect on blood pressure, but it significantly improved baroreflex function in SHR. Treatment with HRS abated oxidative stress, restored antioxidant enzymes including superoxide dismutase, glutathione peroxidase, and catalase, and suppressed NADPH oxidase. Furthermore, treatment with HRS depressed pro-inflammatory cytokines expression including IL-6 and IL-1β and suppressed NF-κB activation, restored mitochondrial function including ATP formation and membrane integrity. In addition, although treatment with HRS had no significant effect on nitric oxide amount in circulating or aorta, it suppressed endothelial nitric oxide synthase expression and upregulated dimethylarginine dimethylaminohydrolase 2 expression in SHR. In conclusion, treatment with HRS alleviates vascular dysfunction through abating oxidative stress, restoring baroreflex function, suppressing inflammation, preserving mitochondrial function, and enhancing nitric oxide bioavailability.

1. Introduction

Vascular dysfunction including endothelial dysfunction and aortic hypertrophy in hypertension often results in poor clinical outcomes and increased risk of vascular accidents [1]. Accumulating studies strongly suggest important pathophysiological roles for increased oxidative stress in the pathological process of vascular dysfunction in hypertensive patients and animals [2]. However, clinical trials with antioxidant vitamin C and E failed to show an improved cardiovascular outcome. Does this mean that antioxidant approaches have no role in prevention or treatment in cardiovascular diseases? In fact, it is clear that the term oxidative stress covers a diverse array of complex biological actions ranging from highly specific redox signaling involving specialized enzymes to interactions with nitric oxide to more straightforward effects such as "damage" to cells, membranes and macromolecules. Therefore, it is hardly surprising that the use of non-specific antioxidants did not produce the desired results. Furthermore, these agents are relatively inefficient and have generally been used without any assessment of the target population for levels of oxidative stress. What may be needed are much more specific agents that can target defined ROS sources and deleterious redox-dependent signal pathways.

Recently, it has been proved that hydrogen gas, a highly flammable gas, has therapeutic antioxidant property by selectively reducing toxic ROS including hydroxyl radical and $ONOO^-$ and protects organs damage such as transient cerebral ischemia, neonatal cerebral hypoxia–ischemia, liver injury and myocardial injury induced by ischemia and reperfusion [3–6]. Apart from

Abbreviations: HRS, hydrogen-rich saline; NF-κB, NF-kappa B; DDAH2, dimethylarginine dimethylaminohydrolase 2; SOD, superoxide dismutase; eNOS, endothelial nitric oxide synthase; GPx, glutathione peroxidase; ROS, reactive oxygen species; SBP, systolic blood pressure; DBP, diastolic blood pressure; HP, heart period; SBPV, systolic blood pressure variability; DBPV, diastolic blood pressure variability; BRS, baroreflex sensitivity; MDA, malondialdehyde; O_2^-, superoxide; $OONO^-$, peroxynitrite; AW, aortic weight; WT, wall thickness; SHR, spontaneously hypertensive rats; WKY, Wistar-Kyoto rats.

* Corresponding author at: Department of Pharmacology, College of Pharmacy, Second Military Medical University, Shanghai 200433, China.
Tel.: +86 21 8187 1270.
E-mail address: yuys1982@hotmail.com (Y.-S. Yu).

[1] Both the authors contributed equally to the work.

0006-2952/$ – see front matter © 2012 Elsevier Inc. All rights reserved.
doi:10.1016/j.bcp.2012.01.031

antioxidant property, hydrogen has potent anti-inflammatory and anti-apoptotic properties [7,8].

Treatment with hydrogen usually utilized two methods including inhalation of hydrogen gas or injection of hydrogen-rich saline (HRS). Compared to hydrogen gas, hydrogen-rich saline is safe, economical and easily available. In addition, hydrogen-rich saline is more convenient for long-term treatment. In the current study, we tested whether long-term treatment with hydrogen-rich saline protected against vascular dysfunction in spontaneously hypertensive rats (SHR) and elucidated the underlying mechanism.

2. Material and methods

2.1. Material

Chemicals, reagents, and drugs were purchased from Sigma Chemical (St. Louis, MO, USA) unless otherwise stated.

2.2. Animals and study design

The 8-week-old male SHR and age-matched normotensive Wistar-Kyoto rats (WKY), with initial body weights of between 200 and 250 g, were purchased from the Sino-British SIPPR/BK Lab Animal Ltd. All the animals were maintained under constant conditions of temperature (23–25 °C) and illumination (light, 08:00–20:00 h; darkness, 20:00–08:00 h). Animals had free access to food and tap water. All the animals used in this work received humane care in compliance with institutional animal care guidelines, and were approved by the Local Institutional Committee. All the surgical and experimental procedures were in accordance with institutional animal care guidelines.

Animals were divided into four groups ($n = 12$ in each group) and treated for 3 months as follows: (1) WKY treated with saline; (2) WKY treated with the HRS; (3) SHR treated with saline; and (4) SHR treated with the HRS. 6 ml/kg of HRS or saline was intraperitoneally injected daily in the morning.

2.3. Hydrogen-rich saline (HRS)

Hydrogen gas was dissolved in physiological saline for 4 h under the pressure of 0.4 MPa as method described by Ohsawa [9]. The saturated hydrogen saline (pH 7.4) was stored under atmospheric pressure at 4 °C in an aluminum bag with no dead volume for use within 1 week. Hydrogen-rich saline was sterilized by gamma radiation. Hydrogen-rich saline was freshly prepared every week to ensure a constant concentration more than 0.6 mM. Gas chromatography was used to confirm the content of hydrogen in saline by the method described [9].

2.4. Blood pressure measurement

Systolic blood pressure (SBP), diastolic blood pressure (DBP), heart period (HP), and heart rate (HR) were recorded continuously as previously described [10]. Briefly, rats were anesthetized with a combination of ketamine (40 mg/kg, i.p.) and diazepam (6 mg/kg, i.p.). A floating polyethylene catheter was inserted into the lower abdominal aorta via the left femoral artery for BP measurement, and another catheter was indwelled in the left femoral vein for intravenous injection. The catheters were exteriorized through the interscapular skin. After a 2-day recovery period, the animals were placed for BP recording in individual cylindrical cages with food and water. The aortic catheter was connected to a BP transducer via a rotating swivel what allows the animals to move freely in the cage. After about 14-h habituation, the BP signals were digitized by a microcomputer, and beat-to-beat SBP, DBP, HR and HP values were determined on line. The mean values of these parameters during the 24 h were calculated and served as SBP, DBP, HR and HP for study. The mean standard deviation over the mean was calculated and defined as the quantitative parameter of blood pressure variability (BPV).

2.5. Baroreflex sensitivity (BRS) measurement

Under above-mentioned BP recording conditions, BRS was measured in conscious rat as previously described [10]. A bolus injection of phenylephrine was given to induce a BP elevation. The dose of phenylephrine was adjusted to raise SBP by 20–40 mmHg. It exist a delay (about 1 s) between the elevation of BP (stimulus) and the prolongation of HP (response) for arterial baroreflex. In rat, the heart rate is about 5 or 6/s. So HP was plotted against SBP for linear regression analysis for 2–8 shifts (calculated by computer); the slope with the largest correlation coefficient of HP/SBP was defined as BRS. The mean of the two measurements with a proper dose served as the final result.

2.6. Morphometric analysis

The thoracic aortae were removed and aortic weight to the length of aorta (AW/length) was calculated. Morphometric analysis of aorta was performed using video microscopy at a final magnification of 100. The image was captured and displayed on a computer monitor using the image analysis software (LEICA QUIPS, LEICA Imaging Systems, UK). Wall thickness (WT) was measured as the distance between endothelium and adventitia.

2.7. Aortic relaxation in response to acetylcholine

Thoracic aortas were removed, cleared of adhering connecting tissue, cut into rings 2 mm in length and placed in Krebs buffer. Protocols were performed on rings beginning at their optimum resting tone, previously determined to be 3 g for rat aorta. This resting tone was reached by stretching rings in 500 mg increments separated by 10-min intervals. Data were collected using a MacLab system and analyzed using Dose Response Software (AD Instruments, Colorado Springs, CO, USA). Vessel rings were preconstricted with phenylephrine (1 μmol/l) (Sigma, St. Louis, MO, USA), and their vasorelaxant dose responses to acetylcholine (1 nmol/l to 10 μmol/l) (Sigma, St. Louis, MO, USA) was recorded. Relaxation to acetylcholine is expressed as a percent relaxation to phenylephrine-induced contraction.

2.8. Measurement of aortic and serum malondialdehyde (MDA)

MDA concentration is a presumptive marker of oxidant-mediated lipid peroxidation. Tissue homogenates and serum were used for the determination of MDA using a kit (Cayman, Ann Arbor, USA). Aortas were removed and homogenized (1:8, w/v) in RIPA buffer (PBS, 1% Nonidet P-40 or Igepal CA-630, 0.5% sodium deoxycholate, 0.1% SDS, and a cocktail of protease inhibitors (Sigma, St. Louis, MO, USA)). The samples were centrifuged at 12,000 × g for 20 min at 4 °C. The supernatant was used for measurement of MDA content.

2.9. Measurement of inflammatory cytokines in serum

Immediately after decapitation, a 2 ml blood sample was collected and serum sample was obtained by centrifugation at 2000 rpm for 15 min and stored at −20 °C for assay within 2 months. Serum IL-1β and IL-6 levels were evaluated using an enzyme-linked immunosorbent assay (ELISA) kit (R&D Systems, Minneapolis, MN, USA). All samples were assayed in duplicate according to the manufacturer's instructions.

2.10. Quantitative real-time PCR analysis

Total RNA was extracted from aorta by using TRIzol (Life Technologies Inc., Gaithersburg, USA) according to the manufacturer's protocol. First-strand cDNA was prepared from total RNA by using SuperScript First-Strand Synthesis Kit (Invitrogen, Carlsbad, USA). To assess genomic DNA contamination, controls without reverse transcriptase were included. Oligonucleotide primers were designed based on the cDNA sequences reported in the GenBank database. The sequences of primers are listed in Table 1. Real-time PCR analysis was performed with a QuantiTectTM SYBR® Green PCR (Tiangen, Shanghai, China) according to the manufacturer's instructions. The highly specific measurement of mRNA was carried out for IL-6, IL-1β, IκBα, NF-κB p65 and GAPDH using the LightCycler system (Bio-Rad, Carlsbad, USA). Each sample was run and analyzed in duplicate. IL-6, IL-1β, IκBα, NF-κB p65 mRNA levels were adjusted as the values relative to GAPDH, which was used as the endogenous control to ensure equal starting amounts of cDNA. The WKY group was used as the calibrator with a given value of 1, and the other groups were compared with this calibrator.

2.11. Western blotting analysis

The protein concentration was determined with BSA as a standard by a Bradford assay. Equal amount of protein preparations (10 μg in 10 μl buffer) were run on SDS-polyacrylamide gels, electrotransferred to polyvinylidine difluoride membranes, and blotted with a primary antibody against dimethylarginine dimethylaminohydrolase 2 (DDAH2, 1:1000, Abcam, Cambridge, UK), eNOS (1:500, Abcam), IκBα (1:500, Abcam), and NF-κB p65 (1:500, Abcam) overnight at 4 °C using slow rocking. Then, they were blotted with HRP-conjugated secondary antibody (1:5000, Sigma) and HRP-conjugated monoclonal antibody against GAPDH (1:10,000, Sigma). Immunoreactive bands were detected by a chemiluminescent reaction (ECL kit, Amersham Pharmacia, USA). The proteins were first normalized to GAPDH and then the other groups were compared with the normalized WKY group.

2.12. Determination of nitrite/nitrate (NOx) content

The levels of NOx, the stable end products of NO, in aortae and serum were measured using a Total Nitrite/Nitrate Assay kit (Dojindo, Kumamoto, Japan) which employed the Griess method. Aortic NOx concentration was calculated as nmol/mg of protein.

Table 1
Sequences of oligonucleotides of the primers.

Target gene	Sequence (5′–3′)	Accession number[a]
IL-6		
Sense	TCCTACCCCAACTTCCAATGCTC	NM_012589
Antisense	TTGGATGGTCTTGGTCCTTAGCC	
IL-1β		
Sense	CACCTCTCAAGCAGAGCACAG	NM_031512
Antisense	GGGTTCCATGGTGAAGTCAAC	
IκBα		
Sense	CCCTGGAAAATCTTCAGACG	NM_001105720
Antisense	ACAAGTCCACGTTCCTTTGG	
NF-κB p65		
Sense	CATCAAGATCAATGGCTACA	NM_199267.2
Antisense	CACAAGTTCATGTGGATGAG	
GAPDH		
Sense	AGACAGCCGCATCTTCTTGT	NM_017008
Antisense	CTTGCCGTGGGTAGAGTCAT	

[a] GenBank accession number of cDNA and corresponding gene is available at http://www.ncbi.nlm.nih.gov/.

2.13. Measurement of SOD activity

Aortic SOD activity was measured using an SOD-525TM reagent kit (OXIS International, Foster, CA, USA).

2.14. NADPH oxidase activity

Lucigenin-enhanced chemiluminescence was used to measure NADPH oxidase activity in aorta according to the method described previously [11].

2.15. Determination of catalase activity in aorta

Catalase activity was measured by the method of Beers and Sizer, as previously described [12].

2.16. Determination of glutathione peroxidase (GPx) activity in aorta

Glutathione peroxidase concentrations were determined in aortic homogenates by using a commercially available kit, according to the manufacturer's protocol (Cayman Chemicals, Ann Arbor, MI, USA).

2.17. Aortic total ROS, O_2^-, and $OONO^-$ production

Aortic total ROS, O_2^-, and $OONO^-$ production was detected as the method described by Elks [13]. Briefly, samples were incubated at 37 °C with 6.6 μl of CMH (1-hydroxy-3-methoxycarbonyl-2,2,5,5-tetramethylpyrrolidine, 200 μM) for 30 min for ROS measurement; CMH for 30 min, then 1.5 μl of PEG-SOD (polyethylene glycol-conjugated superoxide dismutase, 50 U/l) for an additional 30 min for O_2^- measurement; or 30 μl of CPH (1-hydroxy-3-carboxypyrrolidine, 500 μM) for 30 min for $OONO^-$ measurement.

2.18. Measurement of mitochondrial ATP production and ROS formation

Mitochondria were isolated by differential centrifugation of thoracic aortic homogenates as the method described previously [14]. Mitochondrial protein concentration was determined using a DC Protein Assay Kit (Bio-Rad, Hercules, CA, USA). Rates of ATP formation were quantified using a commercially available kit (BioVision, Mountain View, CA, USA). Mitochondrial ROS production was evaluated by lucigenin chemiluminescence. The results were corrected for protein content.

2.19. Measurement of mitochondrial swelling

Measurement of mitochondrial swelling was done by the method of Mariappan [14]. The absorbance was measured at 540 nm.

2.20. Measurement of mitochondrial electron transport chain enzyme activity

The activity of rotenone-sensitive complex I and antimycin A-sensitive complex III were assayed using a thermostatically regulated Thermo-Spectronic spectrophotometer (Fisher Scientific, Epsom, UK).

The activity of complex I (NADH:ubiquinone oxidoreductase) was determined by monitoring the oxidation of NADH at 340 nm. The assay medium contains a mixture of 25 mM potassium phosphate (pH 7.2 at 20 °C), 5 mM $MgCl_2$, 2.5 mg/ml bovine serum albumin, and 2 mM KCN. Baseline activity was established for 1 min after the addition of 0.13 mM NADH,

65 μM ubiquinone, and 2 μg/ml antimycin A. The reaction was initiated by addition of mitochondria (25 μg of protein), and the rate of oxidation of NADH was monitored by the decrease in absorbance at 340 nm and was recorded for 3 min. Rotenone (2 μg/ml) was then added, and the rate of change in absorbance was measured for an additional 3 min. Complex I activity was determined by subtracting the rotenone insensitive activity from the total activity.

The activity of complex III (ubiquinol:cytochrome c oxidoreductase) was determined by monitoring the reduction of ferrocytochrome c at 550 nm. The assay medium is the same as for complex I. 2 mM KCN was included in the assay media to prevent the reoxidation of the product, ferrocytochrome c, by cytochrome c oxidase. Nonenzymatic activity was recorded for 1 min after the addition of 15 μM ferrocytochrome c, 2 μg/ml rotenone, 0.6 mM dodecyl-β-D-maltoside, and 35 μM ubiquinol. The complex III activity was initiated by addition of mitochondrial fraction (10 μg of protein), and the rate of reduction of ferrocytochrome c was recorded for 1 min. Specific complex III activity was calculated by subtracting the antimycin A (2 μg/ml) insensitive activity from the total activity.

2.21. Plasma pH measurement

Plasma pH was determined by using blood-gas analysis in an automatic blood-gas analyzer (ABL system, Radiometer, Copenhagen, Denmark).

2.22. Statistical analysis

Quantitative data were expressed as mean ± SD. To compare the relaxation–response curves, a four parametric logistic model was fit to the dose–response curves. Comparisons of aortic relaxation between groups were made using analysis of variance followed by Student–Newman–Keuls posthoc test. Differences in hemodynamic parameters, serum cytokines, aortic mRNA levels of cytokines, aortic MDA level, ROS formation, aortic NOx level and expressions of DDAH2 and eNOS in aorta between groups were examined using paired *t*-tests. Difference was considered statistically at $p < 0.05$. Statistical analysis was performed by using software SPSS 11.0.0. (SPSS Inc., Chicago, IL, USA).

Table 2
Effects of HRS on body weight, plasma acid–base status, blood pressure, blood pressure variability and baroreflex sensitivity in WKY and SHR.

	WKY	WKY + HRS	SHR	SHR + HRS
BW (g)	383 ± 33	375 ± 37	352 ± 29*	355 ± 32*
Plasma pH	7.51 ± 0.15	7.48 ± 0.16	7.53 ± 0.12	7.50 ± 0.14
SBP (mmHg)	139 ± 15	144 ± 23	189 ± 18*	183 ± 17*
DBP (mmHg)	99 ± 11	96 ± 15	117 ± 13*	115 ± 9*
HR (bpm)	287 ± 28	283 ± 30	356 ± 33*	349 ± 36*
SBPV (mmHg)	8.01 ± 1.73	7.82 ± 1.74	12.09 ± 2.04*	9.67 ± 1.25*,†
DBPV (mmHg)	6.42 ± 1.11	6.69 ± 1.22	8.17 ± 1.06*	7.88 ± 1.12*
BRS (mmHg/ms)	0.71 ± 0.12	0.75 ± 0.17	0.28 ± 0.09*	0.51 ± 0.13*,†

Values are represented as mean ± SD. BW, body weight; SBP, systolic blood pressure; DBP, diastolic blood pressure; HR, heart rate; SBPV, systolic blood pressure variability; DBPV, diastolic blood pressure variability; BRS, baroreflex sensitivity; HRS, hydrogen-rich saline; WKY, Wistar-Kyoto rats; and SHR, spontaneously hypertensive rats.
* $p < 0.05$ versus WKY.
† $p < 0.05$ versus SHR.
n = 10–12 in each group.

3. Results

3.1. Effects of treatment with HRS on the hemodynamic parameters in WKY and SHR

Treatment with HRS had no significant effect on body weight and plasma pH in animals. Compared to WKY, SBP (p = 0.012), DBP (p = 0.007), SBPV (p = 0.034), DBPV (p = 0.027), HR (p = 0.011) in SHR were higher; BRS (p = 0.007) in SHR was lower, which ensured that the animals were qualified. Treatment with HRS had no significant effect on the SBP, DBP, HR, and DBPV; but it reduced SBPV (p = 0.034) and enhanced BRS (p = 0.031) significantly in SHR, indicating that treatment with HRS effectively attenuated baroreflex dysfunction in SHR (Table 2).

3.2. Effects of treatment with HRS on the vascular injury in SHR

Compared to WKY, SHR exhibited aortic hypertrophy, as evidenced by marked increases in the AW/length (Fig. 1A, p = 0.012) and WT (Fig. 1B, p = 0.019). In addition, it was found that endothelium-mediated vascular relaxations of aortae in response to acetylcholine were markedly impaired in SHR compared with WKY (Fig. 1C, p = 0.022). Treatment with HRS in

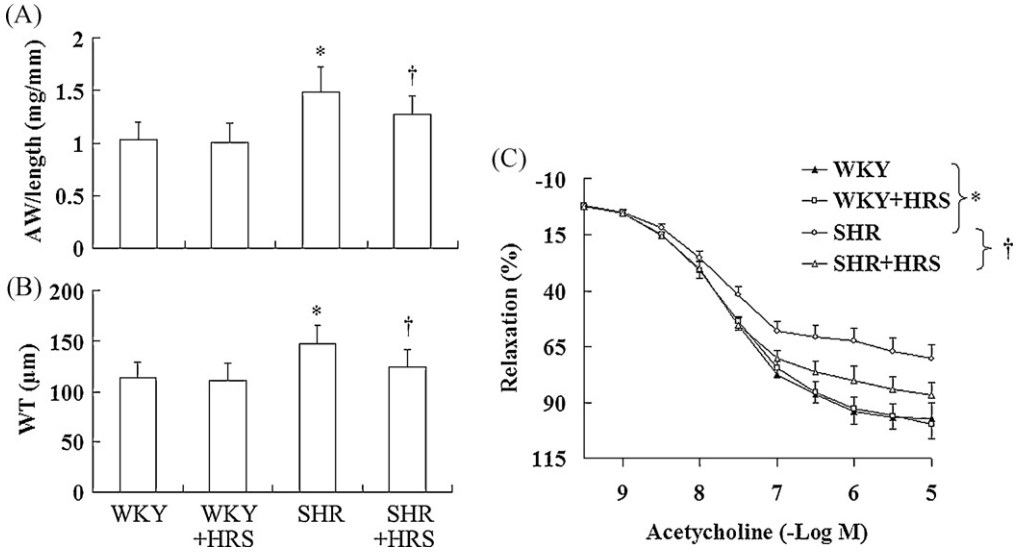

Fig. 1. Effects of HRS on vascular dysfunction in WKY and SHR. Column graphs showed AW/length (A), WT (B) and relaxations to acetylcholine (C) of isolated aorta in WKY and SHR treated with HRS, or not. n = 10–12 in each group. AW, aortic weight; WT, wall thickness; HRS, hydrogen-rich saline; WKY, Wistar-Kyoto rats; and SHR, spontaneously hypertensive rats. *$p < 0.05$ versus WKY; †$p < 0.05$ versus SHR.

Table 3
Effects of HRS on oxidative stress, oxidative stress-related enzymes in WKY and SHR.

	WKY	WKY + HRS	SHR	SHR + HRS
Serum MDA (ng/ml)	3.22 ± 0.78	3.12 ± 0.54	6.41 ± 0.75*	3.96 ± 0.63†
Aortic MDA (nmol/mg protein)	0.76 ± 0.21	0.71 ± 0.17	2.06 ± 0.32*	1.08 ± 0.28†
ROS (μmol/mg protein/min)	0.221 ± 0.042	0.210 ± 0.034	0.462 ± 0.082*	0.287 ± 0.053†
O_2^- (μmol/mg protein/min)	0.0112 ± 0.0023	0.0108 ± 0.0019	0.0827 ± 0.0097*	0.0321 ± 0.0055*,†
$OONO^-$ (nmol/mg protein/min)	5.53 ± 1.09	5.49 ± 1.26	21.7 ± 3.31*	9.65 ± 1.88*,†

Values are represented as mean ± SD. MDA, malondialdehyde; ROS, reactive oxygen species; O_2^-, superoxide; $OONO^-$, peroxynitrite; HRS, hydrogen-rich saline; WKY, Wistar-Kyoto rats; and SHR, spontaneously hypertensive rats.
* $p < 0.05$ versus WKY.
† $p < 0.05$ versus SHR.
n = 10–12 in each group.

SHR decreased AW/length ($p = 0.036$) and WT ($p = 0.039$), and improved endothelium-mediated vascular relaxation ($p = 0.044$) in SHR significantly.

3.3. Effects of treatment with HRS on oxidative stress in SHR

Compared to WKY, MDA content in aorta and serum, total ROS ($p = 0.005$), O_2^- ($p = 0.001$), and $OONO^-$ ($p = 0.003$) production rates in aorta were all significantly higher in SHR. Treatment with HRS resulted in a significant reduction of all of those indexes (total ROS, $p = 0.012$; O_2^-, $p = 0.007$; $OONO^-$, $p = 0.004$). It revealed that treatment with HRS could effectively abate oxidative stress in SHR (Table 3).

3.4. Effects of treatment with HRS on antioxidant enzymes and pro-oxidant enzyme-NADPH oxidase in SHR

SHR exhibited lower activities of aortic SOD (Fig. 2A, $p = 0.007$), GPx (Fig. 2B, $p = 0.006$), and catalase (Fig. 2C, $p = 0.008$), and higher activity of NADPH oxidase (Fig. 2D, $p = 0.002$). Treatment with HRS enhanced SOD ($p = 0.019$), GPx ($p = 0.026$), catalase activities ($p = 0.034$), and suppressed NADPH oxidase activity ($p = 0.031$).

3.5. Effects of treatment with HRS on pro-inflammatory cytokines in SHR

Level of IL-6 (Fig. 3A and B) and IL-1β (Fig. 3C and D) in serum and aorta was significantly higher in SHR than in WKY. Treatment with HRS in SHR resulted in a marked reduction of serum IL-6 (Fig. 3A, $p = 0.027$) and IL-1β (Fig. 3C, $p = 0.031$) concentration, and aortic IL-6 (Fig. 3B, $p = 0.018$) and IL-1β (Fig. 3D, $p = 0.034$) mRNA levels, which revealed that treatment with HRS had a potent anti-inflammatory property.

3.6. Effects of treatment with HRS on NF-κB activation in SHR

Though analysis using the methods of qRT-PCR and Western blotting analysis, it was found that SHR exhibited higher expression of NF-κB p65 (Fig. 4B and D; mRNA, $p = 0.019$; protein, $p = 0.023$) and lower expression of IκBα (Fig. 4A and D; mRNA, $p = 0.002$; protein, $p = 0.008$) in aorta. Treatment with HRS upregulated expression of IκBα (Fig. 4A and D; mRNA, $p = 0.025$; protein, $p = 0.009$) and decreased expression of NF-κB p65 (Fig. 4B and D; mRNA, $p = 0.036$; protein, $p = 0.027$) in aorta of SHR, which revealed that treatment with HRS inhibited NF-κB activation through increasing IκBα expression in SHR.

3.7. Effects of treatment with HRS on mitochondrial function in SHR

Aortic mitochondrial function was impaired in SHR (Fig. 5), as evidenced by marked reduction of activities of complex I (Fig. 5A, $p = 0.016$) and complex III (Fig. 5B, $p = 0.022$), and ATP production (Fig. 5C, indicative of electron transport chain damage, $p = 0.009$), augmentation of ROS formation (Fig. 5D, $p = 0.006$), and increased mitochondrial swelling (Fig. 5E, indicative of membrane damage, $p = 0.026$). Treatment with HRS ameliorated the mitochondrial

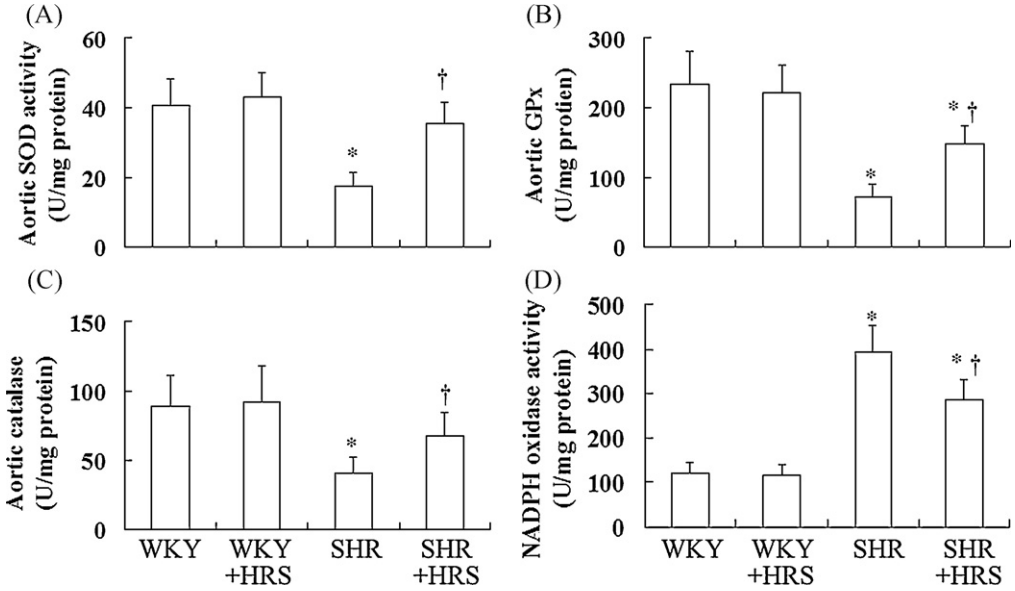

Fig. 2. Effects of HRS on antioxidant enzymes and pro-oxidant enzyme-NADPH oxidase in WKY and SHR. Column graphs showed SOD (A), GPx (B), catalase (C) and NADPH oxidase (D) in aorta of rats. n = 10–12 in each group. SOD, superoxide dismutase; GPx, glutathione peroxidase; HRS, hydrogen-rich saline; WKY, Wistar-Kyoto rats; and SHR, spontaneously hypertensive rats. *$p < 0.05$ versus WKY; †$p < 0.05$ versus SHR.

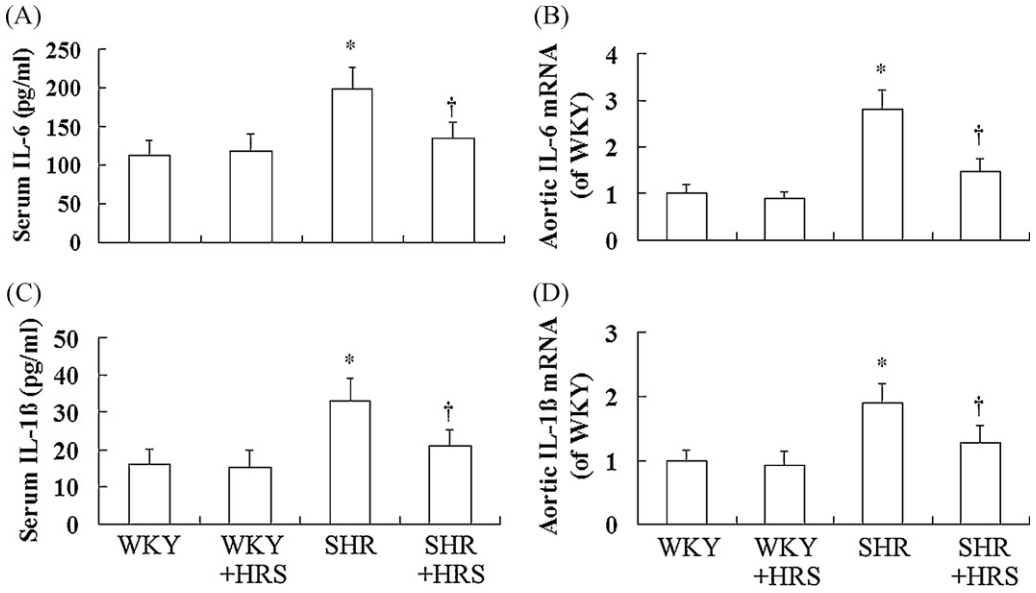

Fig. 3. Effects of HRS on inflammatory cytokines in WKY and SHR. Column graphs showed serum IL-6 concentration (A), aortic IL-6 mRNA level (B), serum IL-1β concentration (C), and aortic IL-1β mRNA level (D) in rats. n = 10–12 in each group. HRS, hydrogen-rich saline; WKY, Wistar-Kyoto rats; and SHR, spontaneously hypertensive rats. $^{*}p < 0.05$ versus WKY; $^{\dagger}p < 0.05$ versus SHR.

dysfunction through decreasing ROS formation ($p = 0.037$), increasing ATP production ($p = 0.040$), and reducing mitochondrial swelling ($p = 0.032$).

3.8. Effects of treatment with HRS on NO formation and related enzymes in SHR

Compared to WKY, NOx (NO_2^- and NO_3^-) levels in aorta (Fig. 6B, $p = 0.019$) and serum (Fig. 6A, $p = 0.012$) were significantly higher in SHR. The eNOS protein expression (Fig. 6C and E, $p = 0.023$) was higher and DDAH2 expression (Fig. 6D and E, $p = 0.031$) was lower in aorta of SHR. As shown in Fig. 6A and B, treatment with HRS had no significant effect on NOx levels in aorta and serum. But, treatment with HRS suppressed eNOS expression ($p = 0.034$) and upregulated DDAH2 expression ($p = 0.007$) in aorta of SHR (Fig. 6C–E).

4. Discussion

In this study, although chronic treatment with HRS had no significant effect on blood pressure, it effectively alleviated endothelial dysfunction and aortic hypertrophy in SHR. Therefore,

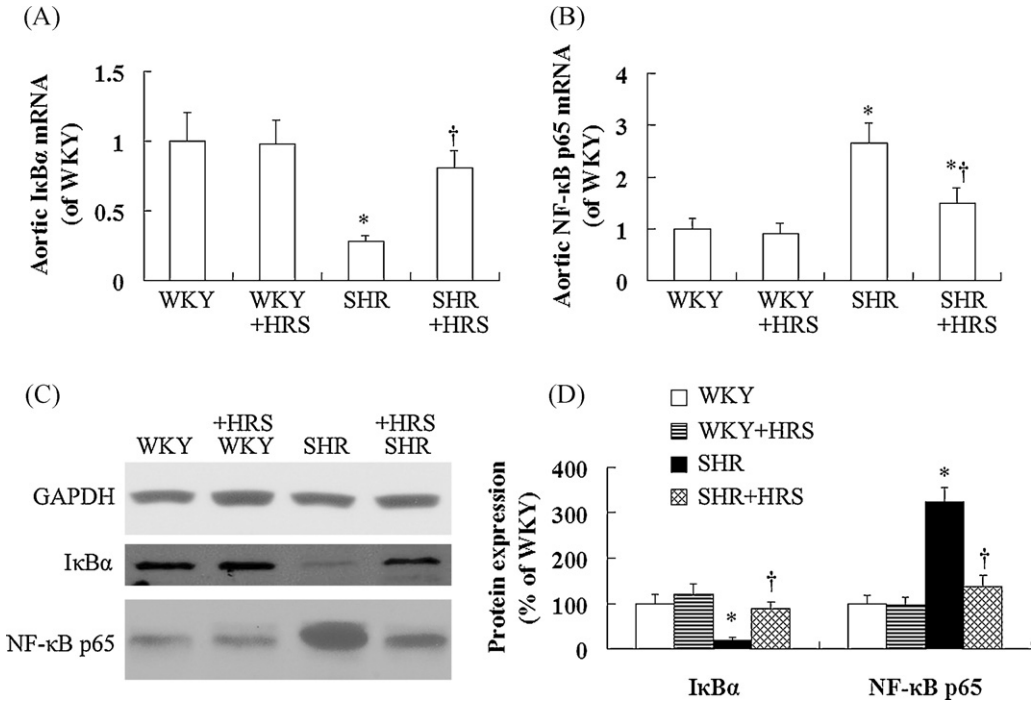

Fig. 4. Effects of HRS on NF-κB activation. Column graphs showed aortic IκBα mRNA (A) and NF-κB p65 mRNA (B). n = 10–12 in each group. Western blotting results (C) and responding quantification of IκBα and NF-κB p65 expression (D) in aorta were showed. Before comparing to WKY, first each IκBα and each NF-κB p65 proteins should be normalized to GAPDH. NF-κB, nuclear factor-kappa B; HRS, hydrogen-rich saline; WKY, Wistar-Kyoto rats; and SHR, spontaneously hypertensive rats. $^{*}p < 0.05$ versus WKY; $^{\dagger}p < 0.05$ versus SHR.

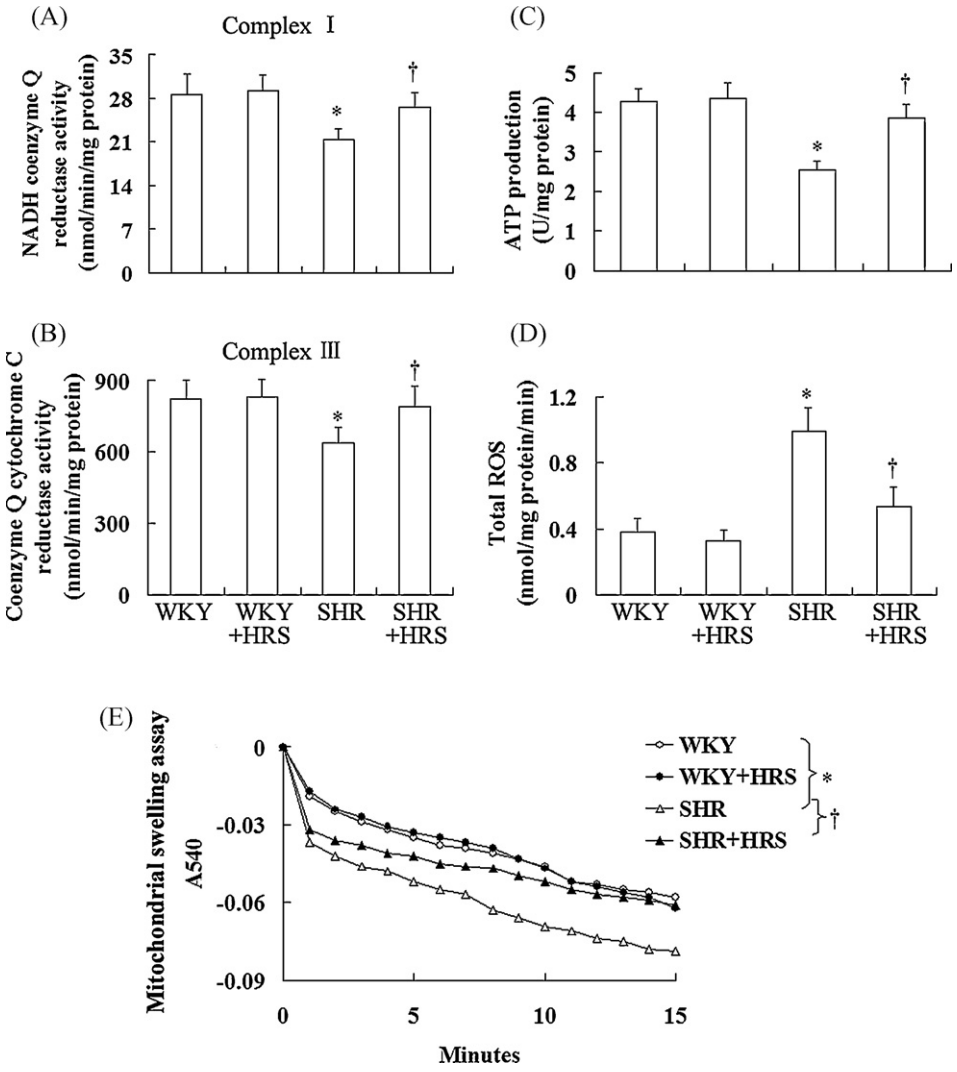

Fig. 5. Effects of HRS on mitochondrial function in WKY and SHR. Graphs showed activity of complex I (A) and complex III (B), ATP formation (C), ROS formation (D), and optical densities for mitochondrial swelling assay (E) in isolated mitochondria of aorta. $n = 10–12$ in each group. HRS, hydrogen-rich saline; ATP, adenosine triphosphate; ROS, reactive oxygen species; WKY, Wistar-Kyoto rats; and SHR, spontaneously hypertensive rats. $^{*}p < 0.05$ versus WKY; $^{\dagger}p < 0.05$ versus SHR.

the beneficial effect of HRS on vascular dysfunction was independent of blood pressure.

Oxidative stress contributed to the development of end organ damages in hypertension including cardiac hypertrophy, vascular dysfunction, and renal damage [15–17]. Oxidative stress describes an imbalance between antioxidant defenses including GPx, SOD, and catalase, and the production of ROS, which at high levels cause cell damage but at lower levels induce subtle changes in intracellular signaling pathways. The major producers of ROS in aorta include plasma membrane-bound NADPH oxidase and mitochondria. In this study, treatment with HRS effectively abated oxidative stress, preserved antioxidant enzymes including SOD, GPx, and catalase, suppressed ROS formation derived from NADPH oxidase and mitochondria. Furthermore, it ameliorated mitochondrial dysfunction, as determined by improved mitochondrial membrane integrity and energy metabolism. The protective effect of HRS on mitochondria might be due to its effect on NADPH oxidase. Several reports have demonstrated that NADPH oxidase-derived ROS lie upstream of mitochondrial-produced ROS, and following mitochondrial dysfunction [18,19]. But since the hydrogen molecule is electrically neutral and much smaller than the other antioxidants, it is able to easily penetrate membranes and enter cells and organelles such as the nucleus and mitochondria, where most commonly-used antioxidant cannot arrive [20]. The unique property of hydrogen might contribute to its beneficial effect on mitochondrial function.

Apart from oxidative stress, inflammation is thought to be another important mediator in the development and progression of vascular dysfunction in hypertensive animals [21,22]. In this study, treatment with HRS significantly decreased pro-inflammatory cytokines including IL-6 and IL-1β in aorta. The anti-inflammatory effect of HRS was also observed in many previous studies [7,23,24]. The anti-inflammatory effect of hydrogen might be secondary to its anti-oxidative effect. Excess ROS activate the redox-sensitive transcription factor NF-κB, resulting in enhancement of its expression and activity [25,26]. Increased expression and activity of NF-κB induces gene transcription of pro-inflammatory cytokines, such as IL-6 and IL-1β, to increase their production [25,27]. In this study, aortic NF-κB activation in SHR was inhibited by treatment with HRS, which might interpret the anti-inflammatory property of HRS, at least in part.

Endothelium-derived NO is a paracrine factor that controls vascular tone, inhibits platelet function, prevents adhesion of leukocytes, and reduces proliferation vascular smooth muscle

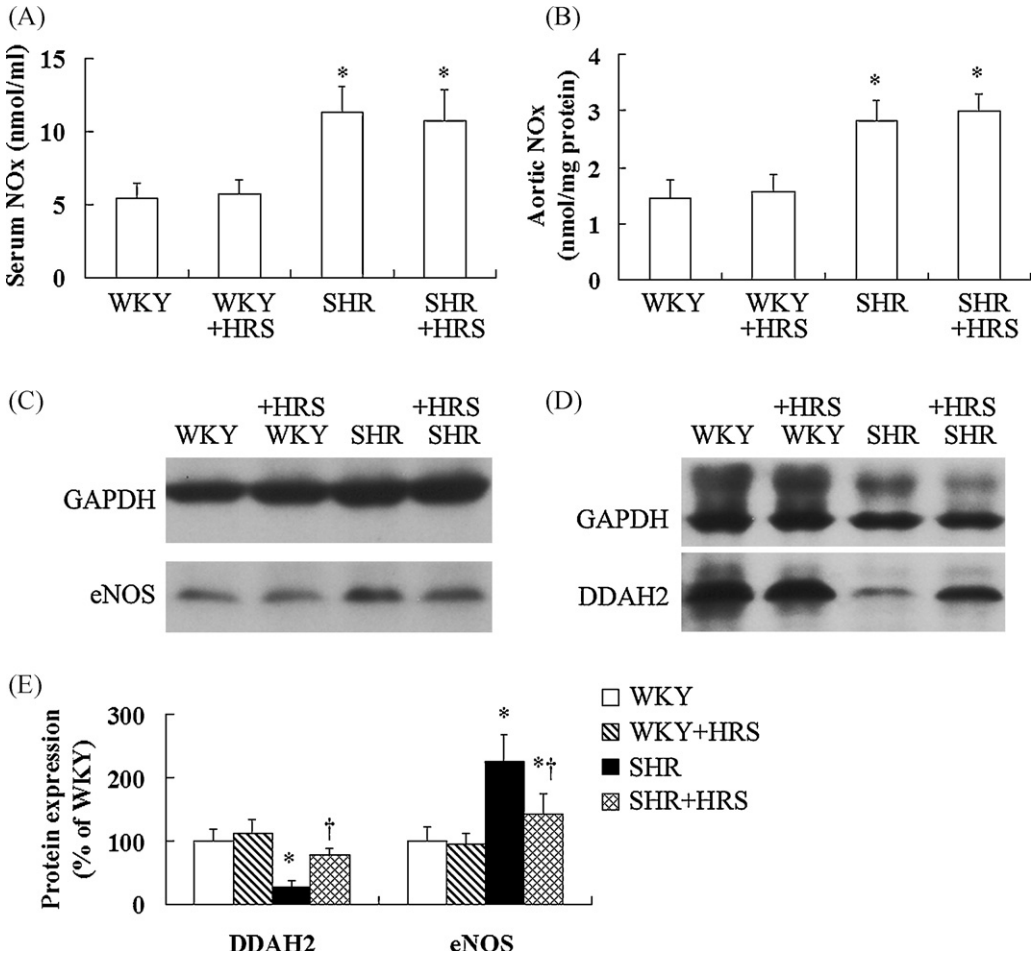

Fig. 6. Effects of HRS on NO formation in WKY and SHR. NOx (NO_2^- + NO_3^-) content in serum (A) and aortae (B) were detected by Griess method. NOx content in aorta was normalized to protein concentration. n = 10–12 in each group. Western blotting results (C, D) and responding quantification (E) of eNOS (C) and DDAH2 (D) expression in WKY and SHR treated with HRS were shown. Before comparing to WKY, first each eNOS and each DDAH2 proteins should be normalized to GAPDH. NO, nitric oxide; eNOS, endothelial nitric oxide synthase; HRS, hydrogen-rich saline; DDAH2, dimethylarginine dimethylaminohydrolase 2; WKY, Wistar-Kyoto rats; and SHR, spontaneously hypertensive rats. $^*p < 0.05$ versus WKY; $^\dagger p < 0.05$ versus SHR.

cells. An enhanced inactivation and/or reduced synthesis of NO is seen in conjunction with risk factors for cardiovascular diseases. Several recent studies have provided evidence for an upregulated eNOS expression in the tissues of young SHR compared with WKY [28,29]. In this study, aortic eNOS expression was also found enhanced in SHR. In addition, aortic DDAH2 expression in SHR was suppressed. DDAH2 is located with eNOS in the cytosol of endothelial cells and responsible for metabolizing asymmetric dimethylarginine, which is an endogenous inhibitor of eNOS [30]. Although total amount of NO in circulating and aorta was elevated, endothelium-dependent relax in SHR was impaired, indicating that aortic NO bioavailability was reduced. Increased ROS could reduce the amount of bioactive NO by chemical inactivation to form toxic $ONOO^-$, which was shown enhanced in aorta of SHR in this study. $ONOO^-$-in turn-could "uncouple" eNOS to become a dysfunction superoxide-generating enzyme that contributes to vascular oxidative stress. In this study, treatment with HRS had no effect on NO amount in plasma and aorta. However, it reduced the excess ROS to elevate NO bioavailability to improve endothelial function. In addition, treatment with HRS was found to suppress eNOS expression and enhance DDAH2 expression in aorta. Several studies in vitro and in vivo demonstrated that an increase in ROS upregulated eNOS expression and suppressed DDAH2 expression [31–33]. Treatment with HRS might restore them by reducing excess ROS in aorta of SHR.

In our present study, another interesting result was that baroreflex function was improved partly by treatment with HRS. Baroreflex is one of the most important mechanisms for cardiovascular regulation, especially in maintaining the stability of blood pressure [34]. It has been recognized that baroreflex function worsens in hypertensive human and animals [35]. Furthermore, it is observed that baroreflex dysfunction was positively related to the severity of organ damages including cardiac hypertrophy, vascular dysfunction and renal damage in hypertensive patients and animals [36]. Animal experiments suggested that decreased BRS is related to increased oxidative stress [37,38]. It is well known that medulla oblongata, including the nucleus tractus solitarus (NTS) and the rostral ventrolateral medulla, plays a crucial role in mediating baroreflex pathway [39,40]. Previous studies demonstrated antioxidants including tempol and vitamin C in the rostral ventrolateral medulla improved baroreflex function [41]. Although it was demonstrated that acute intravenous vitamin C treatment improved baroreflex function in chronic heart failure patients, it was required of very high dose of vitamin C [42]. Since hydrogen is electrically neutral and much small, it can easily penetrate blood–brain barrier and arrive at NTS and RVLM, to exert antioxidant effect.

In conclusion, treatment with HRS alleviates vascular dysfunction in SHR through abating oxidative stress, preserving mitochondrial function, suppressing inflammation, enhancing NO

bioavailability, and restoring baroreflex function. HRS exerts an excellent anti-oxidative effect not only through directly neutralizing with ROS, but also through regulating oxidative-related enzymes. Other effects including preserving mitochondria, suppressing inflammation, enhancing NO bioavailability, and restoring baroreflex function may be secondary to its anti-oxidative effect. However, the underlying mechanism was unclear and required further investigation.

References

[1] Perticone F, Ceravolo R, Pujia A, Ventura G, Iacopino S, Scozzafava A, et al. Prognostic significance of endothelial dysfunction in hypertensive patients. Circulation 2001;104:191–6.
[2] Dhalla NS, Temsah RM, Netticadan T. Role of oxidative stress in cardiovascular diseases. J Hypertens 2000;18:655–73.
[3] Ji Q, Hui K, Zhang L, Sun X, Li W, Duan M. The effect of hydrogen-rich saline on the brain of rats with transient ischemia. J Surg Res 2011;168:e95–101.
[4] Ji X, Liu W, Xie K, Liu W, Qu Y, Chao X, et al. Beneficial effects of hydrogen gas in a rat model of traumatic brain injury via reducing oxidative stress. Brain Res 2010;1354:196–205.
[5] Wang F, Yu G, Liu SY, Li JB, Wang JF, Bo LL, et al. Hydrogen-rich saline protects against renal ischemia/reperfusion injury in rats. J Surg Res 2011;167: e339–44.
[6] Hayashida K, Sano M, Ohsawa I, Shinmura K, Tamaki K, Kimura K, et al. Inhalation of hydrogen gas reduces infarct size in the rat model of myocardial ischemia–reperfusion injury. Biochem Biophys Res Commun 2008;373:30–5.
[7] Zhang Y, Sun Q, He B, Xiao J, Wang Z, Sun X. Anti-inflammatory effect of hydrogen-rich saline in a rat model of regional myocardial ischemia and reperfusion. Int J Cardiol 2011;148:91–5.
[8] Wang C, Li J, Liu Q, Yang R, Zhang JH, Cao YP, et al. Hydrogen-rich saline reduces oxidative stress and inflammation by inhibit of JNK and NF-κB activation in a rat model of amyloid-beta-induced Alzheimer's disease. Neurosci Lett 2011;491:127–32.
[9] Ohsawa I, Ishikawa M, Takahashi K, Watanabe M, Nishimaki K, Yamagata K, et al. Hydrogen acts as a therapeutic antioxidant by selectively reducing cytotoxic oxygen radicals. Nat Med 2007;13:688–94.
[10] Yu YS, Xie HH, Li L, Song SW, Han P, Cai GJ, et al. Effects of low-dose ketanserin on atherosclerosis in rats and rabbits. Can J Physiol Pharmacol 2010;88: 1054–60.
[11] Li YL, Gao L, Zucker IH, Schultz HD. NADPH oxidase-derived superoxide anion mediates angiotensin II-enhanced carotid body chemoreceptor sensitivity in heart failure rabbits. Cardiovasc Res 2007;75:546–54.
[12] Mariappan N, Soorappan RN, Haque M, Sriramula S, Francis J. TNF-α-induced mitochondrial oxidative stress and cardiac dysfunction, restoration by superoxide dismutase mimetic Tempol. Am J Physiol Heart Circ Physiol 2007;293:H2726–37.
[13] Elks CM, Mariappan N, Haque M, Guggilam A, Majid DS, Francis J. Chronic NF-kB blockade reduces cytosolic and mitochondrial oxidative stress and attenuates renal injury and hypertension in SHR. Am J Physiol Renal Physiol 2009;296:F298–305.
[14] Mariappan N, Soorappan RN, Haque M, Sriramula S, Francis J. TNF-α-induced mitochondrial oxidative stress and cardiac dysfunction: restoration by superoxide dismutase mimetic Tempol. Am J Physiol Heart Circ Physiol 2007;293:H2726–37.
[15] Lassegue B, Griendling KK. Reactive oxygen species in hypertension; an update. Am J Hypertens 2004;17:852–60.
[16] Harrison DG, Gongora MC, Guzik TJ, Widder J. Oxidative stress and hypertension. J Am Soc Hypertens 2007;1:30–44.
[17] Laakso J, Mervaala E, Himberg JJ. Increased kidney xanthine oxidoreductase activity in salt-induced experimental hypertension. Hypertension 1998;32: 902–6.
[18] Doughan AK, Harrison DG, Dikalov SI. Molecular mechanisms of angiotensin II-mediated mitochondrial dysfunction: linking mitochondrial oxidative damage and vascular endothelial dysfunction. Circ Res 2008;102:488–96.
[19] Zimmerman MC, Zucker IH. Mitochondrial dysfunction and mitochondrial-produced reactive oxygen species: new targets for neurogenic hypertension. Hypertension 2009;53:112–4.
[20] Maher P, Salgado KF, Zivin JA, Lapchak PA. A novel approach to screening for new neuroprotective compounds for the treatment of stroke. Brain Res 2007;1173:117–25.
[21] Savoia C, Schiffrin EL. Inflammation in hypertension. Curr Opin Nephrol Hypertens 2006;15:152–8.
[22] Sun L, Gao YH, Tian DK, Zheng JP, Zhu CY, Ke Y, et al. Inflammation of different tissues in spontaneously hypertensive rats. Sheng Li Xue Bao 2006;58:318–23.
[23] Gharib B, Hanna S, Abdallahi OMS, Lepidi H, Gardette B, Reggi MD. Anti-inflammatory properties of molecular hydrogen, investigation on parasite-induced liver inflammation. Life Sci 2001;324:719–24.
[24] Kajiya M, Silva MJ, Sato K, Ouhara K, Kawai T. Hydrogen mediates suppression of colon inflammation induced by dextran sodium sulfate. Biochem Biophys Res Commun 2009;386:11–5.
[25] Janssen-Heininger YMW, Poynter ME, Baeuerle PA. Recent advances towards understanding redox mechanisms in the activation of nuclear factor κB. Free Radic Biol Med 2000;28:1317–27.
[26] Schreck R, Rieber P, Baeuerle PA. Reactive oxygen intermediates as apparently widely used messengers in the activation of the NF-κB transcription factor and HIV-1. EMBO J 1991;10:2247–58.
[27] Sanlioglu S, Williams CM, Samavati L, Butler NS, Wang G, McCray PB, et al. Lipopolysaccharide induces Rac1-dependent reactive oxygen species formation and coordinates tumor necrosis factor-alpha secretion through IKK regulation of NF-kappa B. J Biol Chem 2001;276:30188–98.
[28] Vaziri ND, Ni Z, Oveisi F. Upregulation of renal and vascular nitric oxide synthase in young spontaneously hypertensive rats. Hypertension 1998;31: 1248–54.
[29] Akiba Y, Yamaguchi N, Amano H, Fujii T, Fujimoto K, Suzuki T, et al. Role of nitric oxide in control of blood pressure in young and adult spontaneously hypertensive rats. Clin Exp Pharmacol Physiol 1995;22:S142–3.
[30] Anthony S, Leiper J, Vallance P. Endogenous production of nitric oxide synthase inhibitors. Vasc Med 2005;10:S3–9.
[31] Cao P, Ito O, Guo Q, Ito D, Muroya Y, Rong R, et al. Endogenous hydrogen peroxide up-regulates the expression of nitric oxide synthase in the kidney of SHR. J Hypertens 2011;29:1167–74.
[32] Luo Z, Teerlink T, Griendling K, Aslam S, Welch WJ, Wilcox CS. Angiotensin II and NADPH oxidase increase ADMA in vascular smooth muscle cells. Hypertension 2010;56:498–504.
[33] Zhen J, Lu H, Wang XQ, Vaziri ND, Zhou XJ. Upregulation of endothelial and inducible nitric oxide synthase expression by reactive oxygen species. Am J Hypertens 2008;21:28–34.
[34] Su DF, Chen L, Kong XB, Cheng Y. Determination of arterial baroreflex-blood pressure control in conscious rats. Acta Pharmacol Sin 2002;23:103–9.
[35] Su DF, Cerutti C, Barres C, Vincent M, Sassard J. Blood pressure and baroreflex sensitivity in conscious hypertensive rats of Lyon strain. Am J Physiol 1986;251:H1111–17.
[36] Su DF, Miao CY. Blood pressure variability and organ damage. Clin Exp Pharmacol Physiol 2001;28:709–15.
[37] Rabelo E, De Angelis K, Bock P, Gatelli Fernandes T, Cervo F, Belló Klein A, et al. Baroreflex sensitivity and oxidative stress in adriamycin-induced heart failure. Hypertension 2001;38:576–80.
[38] Gouty S, Regalia J, Cai F, Helke CJ. Alpha-lipoic acid treatment prevents the diabetes-induced attenuation of the afferent limb of the baroreceptor reflex in rats. Auton Neurosci 2003;108:32–44.
[39] Dampney RAL, Polson JW, Potts PD, Hirooka Y, Horicuchi J. Functions organization of brain pathways subserving the baroreceptor reflex: studies in conscious animal using immediate early gene expression. Cell Mol Neurobiol 2003;23:597–616.
[40] Schreihofer AM, Guyenet PG. The baroreflex and beyond of sympathetic vasomotor tone by GABAergic neurons in the ventrolateral medulla. Clin Exp Pharmacol Physiol 2002;29:514–21.
[41] Campos RR, Oliveira-Sales EB, Nishi EE, Boim MA, Dolnikoff MS, Bergamaschi CT. The role of oxidative stress in renovascular hypertension. Clin Exp Pharmacol Physiol 2011;38:144–52.
[42] Nightingale AK, Blackman DJ, Field R, Glover NJ, Pegge N, Mumford C, et al. Role of nitric oxide and oxidative stress in baroreceptor dysfunction in patients with chronic heart failure. Clin Sci 2003;104:529–35.